

Beam pen lithography based on focused laser diode beam with single microlens fabricated by excimer laser

Md. Nazmul Hasan and Yung-Chun Lee*

Department of Mechanical Engineering, National Cheng Kung University, Tainan, 701, Taiwan
*yunglee@mail.ncku.edu.tw

Abstract: A method is proposed to minimize the focused spot size of an elliptically-diverging laser diode beam by means of a circular aperture and a single plano-convex aspherical microlens. The proposed microlens is fabricated using an excimer laser dragging method and has two different profiles in the x- and y-axis directions. The focused spot size of the beam is examined both numerically and experimentally. The feasibility of the proposed approach for beam pen lithography applications is demonstrated by patterning dotted, straight-line and spiral features on a photo resist layer followed by thin gold layer deposition and metal lift-off. The minimum feature size for dotted pattern is around 2.57 μm , while the minimum line-widths for straight-line and spiral pattern are 3.05 μm and 4.35 μm , respectively. Thus, the technique can be applied to write any arbitrary pattern for high-resolution lithography.

© 2015 Optical Society of America

OCIS codes: (140.2020) Diode lasers; (140.2180) Excimer lasers; (220.0220) Optical design and fabrication.

References and links

1. Y. Lin, M. H. Hong, T. C. Chong, C. S. Lim, G. X. Chen, L. S. Tan, Z. B. Wang, and L. P. Shi, "Ultrafast-laser-induced parallel phase-change nanolithography," *Appl. Phys. Lett.* **89**(4), 041108 (2006).
2. J. Yang, F. Luo, T. S. Kao, X. Li, G. W. Ho, J. Teng, X. Luo, and M. Hong, "Design and fabrication of broadband ultralow reflectivity black Si surfaces by laser micro/nanoprocessing," *Light Sci. Appl.* **3**(7), e185 (2014).
3. S. W. Tsai, P. Y. Chen, and Y. C. Lee, "Fabrication of a seamless roller mold with wavy microstructures using mask-less curved surface beam pen lithography," *J. Micromech. Microeng.* **24**(4), 045022 (2014).
4. M. Pospiech and S. Liu, *Laser diodes. An introduction* (University of Hannover, 2014).
5. J. Alda, "Laser and Gaussian beam propagation and transformation," in *Encyclopedia of Optical Engineering*, Dekker, ed. (CRC, 2003).
6. H. Sun, *Laser Diode Beam Basics, Manipulations and Characterizations* (Springer, 2012), Chap.3.
7. S. Y. Huang and C. Gaebe, "Astigmatic compensation for an anamorphic optical system," U.S. Patent 6,301,059 (9 October 2001).
8. S. D. Fantone, "Anamorphic prism: a new type," *Appl. Opt.* **30**(34), 5008–5009 (1991).
9. LaserDiodeTechNote1Rev2," (Accessed November 20, 2014).
<http://www.coherent.com/Downloads/LaserDiodeTechNote1Rev2.pdf>.
10. S. H. Wang, C. J. Tay, C. Quan, and H. M. Shang, "Collimating of diverging laser diode beam using graded-index optical fiber," *Opt. Lasers Eng.* **34**(2), 121–127 (2000).
11. J. J. Snyder, "Microoptic lenses," U.S. Patent 5,181,224 (19 January 1993).
12. X. Q. Zhou, B. N. Ann, and K. S. Seong, "Single aspherical lens for deastigmatism, collimation, and circularization of a laser beam," *Appl. Opt.* **39**(7), 1148–1151 (2000).
13. M. Serkan and H. Kirkici, "Optical beam-shaping design based on aspherical lenses for circularization, collimation, and expansion of elliptical laser beams," *Appl. Opt.* **47**(2), 230–241 (2008).
14. S. Mukhopadhyay, S. Gangopadhyay, and S. Sarkar, "Coupling of a laser diode to a monomode elliptic-core fiber via a hyperbolic microlens on the fiber tip: efficiency computation with the *ABCD* matrix," *Opt. Eng.* **46**(2), 025008 (2007).
15. J.-Y. Hu, C.-P. Lin, S.-Y. Hung, H. Yang, and C.-K. Chao, "Semi-ellipsoid microlens simulation and fabrication for enhancing optical fiber coupling efficiency," *Sens. Actuator A-Phys.* **147**(1), 93–98 (2008).

16. A. Bose, S. Gangopadhyay, and S. C. Saha, "Laser diode to single mode circular core graded index fiber excitation via hemispherical microlens on the fiber tip: identification of suitable refractive index profile for maximum efficiency with consideration for allowable aperture," *J. Opt. Commun.* **33**(1), 15–19 (2012).
17. L. Mi, S. L. Yao, Q. Li, and F. Gao, "Shaping semiconductor laser beam with one-dimension gradient-index lens," in *Journal of Physics: Conference Series*, (IOP Publishing, 2006), pp. 785.
18. DL5146-101S - 405 nm, 40 mW, Ø5.6 mm, B Pin Code, Sanyo Laser Diode," (Accessed November 20, 2014), <http://www.thorlabs.hk/thorproduct.cfm?partnumber=DL5146-101S>.
19. L. L. C. Radiant Zemax, *ZEMAX Optical design program, User's Guide* (ZEMAX Development Corporation, 2000), Chap.14.
20. E. Hecht, "Resolution of imaging system," in *Optics* (Addison-Wesley, 2002), Chap.10.
21. N. H. Rizvi, "Production of novel 3D microstructures using excimer laser mask projection techniques," *Proc. SPIE* **3680**, 546–552 (1999).
22. K. Zimmer, D. Hirsch, and F. Bigl, "Excimer laser machining for the fabrication of analogous microstructures," *Appl. Surf. Sci.* **96–98**, 425–429 (1996).
23. N. H. Rizvi, P. T. Rumsby, and M. C. Gower, "New developments and applications in the production of 3D microstructures by laser micromachining," *Proc. SPIE* **3898**, 240–249 (1999).
24. H. Hocheng and K. Y. Wang, "Analysis and fabrication of minifeature lamp lens by excimer laser micromachining," *Appl. Opt.* **46**(29), 7184–7189 (2007).
25. S. Y. Wang, C.-S. Huang, H.-Y. Chou, T.-Y. Lee, and R.-S. Chang, "Improvement on the surface roughness of micro lens array in the excimer laser machining process," *Proc. SPIE* **4561**, 131–138 (2001).
26. C. C. Chiu and Y. C. Lee, "Excimer laser micromachining of aspheric microlens arrays based on optimal contour mask design and laser dragging method," *Opt. Express* **20**(6), 5922–5935 (2012).

1. Introduction

Laser lithography is widely applied nowadays to pattern nanoscale features on a wafer. One example is phase change nano-lithography where femto-second laser with microlens array is used to fabricate sub-100 nm feature size three dimensional (3D) nano patterns in phase change films [1]. Another is laser interference lithography where He-Cd laser is used to fabricate 3D silicon nano-wire arrays with a diameter of around 300 nm [2]. In mask-less beam pen lithography, wavy patterns are created on a curved surface by translating the microlens array and substrate in a programmable way during UV exposure [3]. Laser diode arrays have significant potential for use as UV light sources since each diode can be controlled individually, thereby allowing the patterning of complex features over a large area. Laser diodes have many advantages over other laser systems, including a compact size, low cost, high electrical-to-laser power conversion efficiency, direct excitation with small electric currents, modulation to the gigahertz order, and the potential for battery operation [4]. They are thus widely used for optical communications, data recording and reading, sensing and measurement, laser printing and so on. However, edge-emitting laser diodes have two point sources (so called astigmatism), which create an elliptical shape of the output beam and large divergence angles in the two transverse directions [5]. These beam characteristics can pose serious problems in some practical applications. For example, astigmatism creates problems for optical data storage systems, while ellipticity and divergence must be corrected for optical read-write head applications. Consequently, some forms of beam manipulation are required.

The literature contains many proposals to solve the astigmatism, ellipticity and divergence problems of laser diodes. For example, in [6, 7] two orthogonally-positioned cylindrical lenses were used to correct astigmatism and convert the elliptical beam into a circular beam. In [6, 8], an anamorphic prism pair was used to circularize the beam and to correct astigmatism with minimum power loss. In [9, 10], a single-mode graded-index optical fiber coupled with a pair of aspherical lenses was used to circularize the elliptical beam, correct astigmatism, and deliver the beam. The authors in [6, 11] showed that by inserting a single micro-cylindrical lens inside the diode cap, the output beam diverged circularly and the astigmatism was corrected. It was shown in [12], that a single aspherical lens with four different profiles of the input and output surfaces could solve all three problems. Meanwhile, two optical designs based on aspherical lenses is demonstrated in [13] to circularize, collimate and expand the beam for LIDAR application.

For beam pen lithography applications, astigmatism and ellipticity are not a concern. However, the divergent beam should be focused so as to minimize the spot size and to achieve the maximum possible pattern resolution on the substrate. In practice, this can be achieved by combining the above methods with one or more additional lenses. However by doing so, the module size, assembly cost and lens manufacturing cost increase. In [14–17], the beam was focused directly using various single lenses, including hyperbolic, semi-ellipsoid, hemispherical and gradient-index. However, these methods are all designed specifically to couple the laser diode beam with single mode fibers.

Accordingly in this paper, a method is proposed to focus and minimize a highly-divergent, elliptical-shaped laser diode beam using a circular aperture and a single plano-convex aspherical microlens with two different profiles of the output surface in the x- and y-axis directions. The propagation characteristics of the laser diode beam and the optimum lens profile are evaluated by means of Zemax ray-tracing simulation. The microlens is then fabricated using an excimer laser dragging method. The focused spot size is examined both numerically and experimentally. Importantly, the aperture and microlens are simply adhered to the laser diode using commercial glue. Consequently, the assembly cost is reduced and the need for expensive alignment apparatus is removed. Finally using the smallest focused spot, three different types of feature (dotted, straight-line and spiral) are demonstrated in the beam pen lithography process.

2. Design and optimization of aspherical microlens

Unlike other laser systems, laser diode beams have an elliptical shape with different divergence angles in the fast and slow axis directions. As a result, circular apertures are required to circularize the output beam by clipping it in the fast axis direction. Importantly, this gives the opportunity to focus the beam directly using a single lens. However, the Gaussian intensity distribution of the circularized output beam is different in both directions. Thus, the aspherical plano-convex microlens proposed in this study is designed with two different profiles in the x- and y- axis directions to properly focus the beam in both directions. To optimize the microlens profile, it is first necessary to understand the laser diode characteristics and beam propagation behavior. As described in the following sub-sections, the characteristics of the diode and beam are modeled by simulation, and the results are then used for a further simulation to optimize the microlens profile.

A. Laser diode characteristics and beam propagation

In the present study, the laser diode characteristics and beam propagation behavior are modeled using Zemax ray-tracing software (ZEMAX Development Co., San Diego, USA). The simulation considers a DL5146-101S laser diode (SANYO Electric Co., Tokyo, Japan) since its wavelength is compatible with common beam pen lithography applications. According to the manufacturer's specification, the diode has a wavelength of 405 nm and divergence angles at FAHM (full-angle-at-half-magnitude) of 8° and 19° in the fast- and slow-axis directions, respectively [18]. Note that, the divergence angles are converted at $1/e^2$ intensity value of 13.6° and 32.3° in the fast- and slow-axis directions, respectively.

In implementing the sequential mode of Zemax, the first source point P_x , which lies on the slow axis, was fixed with an object space NA equal to $\sin(13.6^\circ/2)$. Meanwhile, in the lens data editor, a Paraxial XY surface with a Y-power equal to $470 \mu\text{m}^{-1}$ was inserted to fix the second source point P_y , which lies on the fast axis. For index-guided mode edge-emitting laser diodes, the astigmatic value lies between 5 and $15 \mu\text{m}$ [9]. From simulation, the astigmatism was found as $10.3 \mu\text{m}$. Figure 1(a) shows the simulated point sources and astigmatism of the considered laser diode.

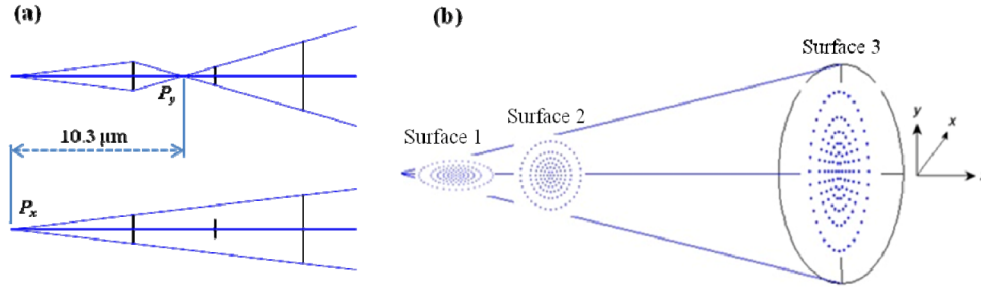


Fig. 1. (a) Astigmatism between two point sources P_x and P_y . (b) Beam propagation along z-axis direction.

As described above, laser diode beams are characterized by astigmatism, elliptical shape, and different divergence angles. Consequently, the beam is elliptical at the emission strip with the major diameter lying along the x-axis. However, within a distance of several microns from the emission strip, the elliptical shape of the beam changes to a circular shape. The beam then returns to an elliptical shape with the major diameter lying along the y-axis in the far field. In the present simulation, the change in the beam shape was modeled by inserting three standard surfaces in the lens data editor. As shown in Fig. 1(b), surface-1 has an elliptical shape with the major diameter in x-axis, surface-2 has a circular shape, and surface-3 is elliptical with the major diameter lying along the y-axis.

B. Design and optimization of microlens profile

The elliptical beam size at the position of the diode window cap was found from the Surface-3 to be $596.8 \mu\text{m}$ in the fast-axis direction and $247.9 \mu\text{m}$ in the slow-axis direction. Since the beam diverges elliptically, a stainless steel circular aperture with a thickness of $50 \mu\text{m}$ (Ten Sun Development Company, Tainan, Taiwan) was used to make the beam diverge circularly by clipping it in the fast axis. Based on the simulation results, the aperture diameter was chosen as $260 \mu\text{m}$ such that the beam intensity was reduced only in the fast-axis direction. The transmission loss induced by the aperture was calculated to be 21.73%.

In the proposed focusing method, a plano-convex microlens was placed such that the plano surface was in contact with the circular aperture. A polycarbonate material (CT301310, Goodfellow Cambridge Ltd., Huntingdon, England) was chosen for the microlens, which had a thickness of $175 \mu\text{m}$, a refractive index of 1.63 and an Abbe number of 34. Moreover, the lens diameter was specified as $300 \mu\text{m}$ to ensure that all the light emitted from the circular aperture passed through the lens, as shown in Fig. 2.

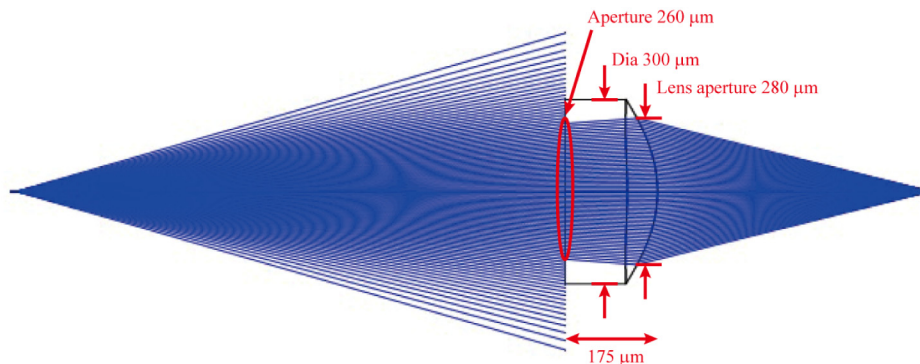


Fig. 2. Circular aperture used to circularize the output beam and microlens used to achieve the minimum focused spot size.

To optimize the design of the plano-convex microlens, the profile of the convex surface was modeled using the polynomial sag height function given in Eq. (1) [19]. In general, the use of a polynomial function has three main advantages, namely (1) it enables the design of different lens profiles in the x- and y-axis directions; (2) it makes possible the realization of complex surface patterns and (3) it is compatible with the excimer laser dragging method used in the present study, in which dragging along the two transverse directions is separately controlled (see Section 3).

$$Z(x,y)=\gamma_1x^2+\gamma_2x^4+\gamma_3x^6+\gamma_4x^8+\gamma_5y^2+\gamma_6y^4+\gamma_7y^6+\gamma_8y^8, \quad (1)$$

where $Z(x,y)$ is the sag height of the cross-section profile of the polynomial surface at any radius and γ_1 to γ_8 are polynomial coefficients representing the second to eighth even-order terms. More specifically, coefficients γ_1 to γ_4 control the lens profile in the x-axis direction while coefficients γ_5 to γ_8 control the lens profile in the y-axis direction.

In performing the optimization process, the coefficient values were adjusted in such a way to minimize the focused spot size. The optimization process was based on a default Merit Function specified in terms of the “RMS” and “Spot X+Y” parameters, where RMS is the Root-Mean-Square of all the individual errors and Spot X + Y is the x and y extent of the transverse ray aberration. After the optimization process, the Airy disk, which represents the diffraction limited spot [20], showed that the optimal lens profile had an elliptical shape with a diameter of $3.99 \mu\text{m}$ at a focal length of 1.98 mm. It is noted that this ellipticity is not a concern in beam pen lithography since the spot size is very small.

The total intensity distribution over the focal plane was computed in the x- and y-axis directions of the airy disk using the “FFT PSF cross section”, in which the $1/e^2$ or FWHM (full-width-at-half-magnitude) intensity diameters were calculated at normalized intensities of 0.135 and 0.5, respectively. The focused spot sizes in the x- and y-axis directions were found to be $5.32 \mu\text{m}$ and $4.97 \mu\text{m}$, respectively, as shown in Fig. 3. Table 1 represents the values of the eight coefficients in the sag height function (see Eq. (1)) for the optimized microlens profile. Figure 4 shows the sag height profiles obtained by plotting Eq. (1) using the optimal coefficients values given in Table 1. It is seen that the maximum sag heights in the x-axis (0°) and y-axis (90°) directions are $23.15 \mu\text{m}$ and $23.27 \mu\text{m}$, respectively.

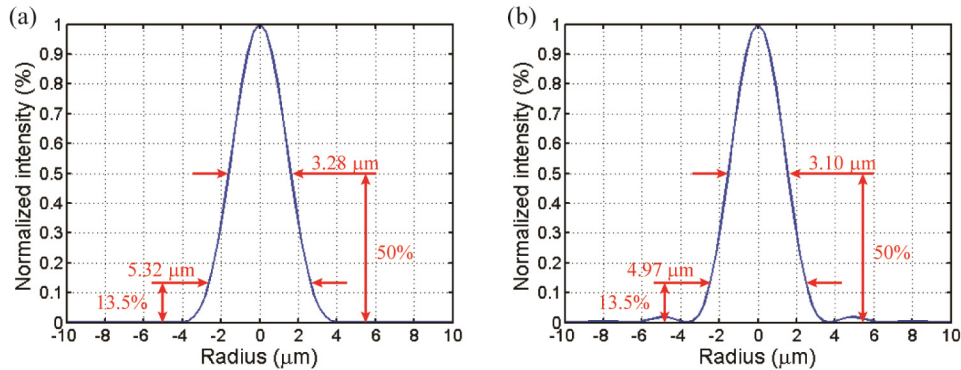


Fig. 3. Light intensity distribution at focal plane and focused spot sizes. (a) Spot size at 13.5% and 50% intensity in x-axis (b) Spot size at 13.5% and 50% intensity in y-axis.

Table 1. Eight coefficients for x and y profiles of aspherical lens polynomial surface.

Coefficients	γ_1	γ_2	γ_3	γ_4
x profile	-1.028804	-0.01345	0.669652	0.0
Coefficients	γ_5	γ_6	γ_7	γ_8
y profile	-1.034665	0.014509	-0.163106	0.0

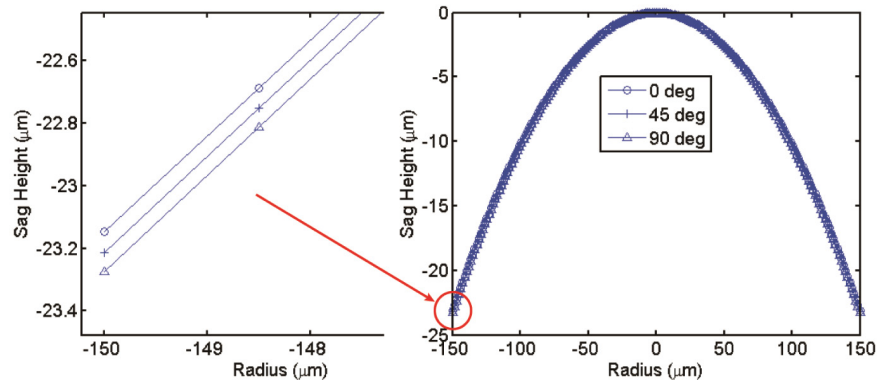


Fig. 4. Microlens profiles indicate difference of sag height at different angles, where the sag heights at different angles are enlarged in left-hand figure.

3. Microlens fabrication and assembly

A. Fabrication of microlens by excimer laser dragging method

The optimized aspherical microlens was fabricated using an excimer laser micromachining system in which both the pulse duration and the pulse repetition rate can be controlled. In general, the machining process can be performed by dragging either the object or the contour mask continuously along one direction as the laser fires. Previous studies have shown that given an appropriate mask profile, micro-channels or micro-grooves can be produced using a contour mask scanning method [21]. The contour mask is a binary photo-mask containing a specially-designed pattern, which allows laser light to pass through as it is dragged along a programmed scanning path such that the overall or overlapped laser energy projected on the sample surface satisfies a certain spatial distribution [22]. If the contour mask contains periodic patterns which are used in two straight and orthogonal laser dragging paths, it is possible to create arrayed 3D microstructures in a process known as excimer laser dragging method [23–25]. During the dragging process, each laser pulse removes a constant depth of material from the sample surface. Thus, the machining depth of the microlens is proportional to the number of laser shots at a particular point. In practice, the desired lens profile depends on the contour mask design, the laser energy and the separation distance between successive laser pulses. Following the first laser dragging pass along one direction, a 2D surface profile similar to that of a cylindrical lens is created. A second laser dragging pass in a direction perpendicular to the first is then performed to superimpose an additional machining depth in the overlapping area with the first pass, resulting in the desired 3D surface profile.

The excimer laser dragging system used in the present study was based on a COMPex Pro 210 (Lambda Physik, Germany) laser source with a wavelength of 248 nm (KrF). (Full details of the excimer laser micromachining system and the machining method are available in [26].) Notably, the authors in [26] used an aspherical surface function to describe the contour mask pattern required to machine an aspherical lens profile. However, despite optimizing the function using the Simplex method, a small axial symmetrical error was observed in the simulated lens. By contrast, using the polynomial surface function describe in Eq. (1), single or double contour mask patterns for any lens profile can be developed, which ensures that the lens has no such error. Moreover, the contour mask patterns $h(x)$ and $h(y)$ defined using the polynomial surface function are compatible with the excimer laser fabrication technique used in this study, in which dragging is performed separately in the x- and y-axis directions, as shown in Fig. 5(a). Furthermore, from Eq. (1), it is clear that the sag height of the polynomial surface function represents the addition of two masks. Thus, the polynomial surface function can be applied to generate any lens profile, including semi-circular, cylindrical or elliptical.

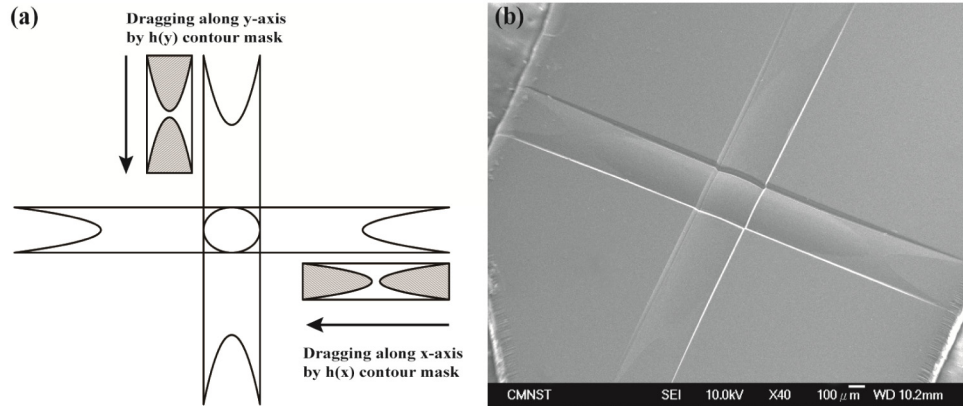


Fig. 5. (a) Schematic diagram showing fabrication of single microlens using two contour masks $h(x)$ and $h(y)$. (b) SEM image of a fabricated microlens.

A polycarbonate (PC) sheet with a thickness of $175\ \mu\text{m}$ was used as the microlens material since PC has good optical properties and a smooth surface after excimer laser machining. The machining rate ($\mu\text{m}/\text{pulse}$) was determined experimentally. At a laser fluence of around $200\ \text{mJ}/\text{cm}^2$, the machining rate was found to be $0.1\ \mu\text{m}/\text{pulse}$. Once the machining rate was determined, the relative laser firing interval was chosen in such a way to achieve the desired machining depth and surface profile. For example, given a laser-machining rate of $5\ \text{Hz}$ and a separation distance between two successive laser shots of $2\ \mu\text{m}$, the sample moving speed was set as $10\ \mu\text{m}/\text{sec}$. The total machining time to fabricate a single aspherical microlens was around 6 minutes. Figure 5(b) shows a Scanning Electron Microscope (SEM) image of the fabricated microlens.

B. Evaluation of the fabricated microlens

The surface profile of the fabricated microlens was measured using a color non-contact 3D topography laser scanning system (VK 9700, Keyence Ltd., Osaka, Japan). Figures 6(a) to 6(c) compare the 2D cross-section profiles of the fabricated and simulated microlens along the 0° , 45° and 90° directions relative to the x-axis. It is observed that an excellent agreement exists between the two sets of results in every case. At a distance more than $140\ \mu\text{m}$ from the lens center, there exists a small profile error in the 0° and 90° directions. However, for the 45° direction, no profile error or axial symmetrical error is observed. Figures 7(a) to 7(c) shows the difference between the fabricated surface profile data and the simulated data at angles of 0° , 45° and 90° with respect to the x-axis. The results confirm that the machined surface profile is accurate in the central region of the lens. However, small errors are observed at the lens edge. As shown in Fig. 2, the light passes through the central region of the lens with a radius of $140\ \mu\text{m}$. The maximum profile error within this region of the lens is seen from Fig. 7 to be just $\pm 0.4\ \mu\text{m}$. Thus, the feasibility of the biaxial laser dragging method with a polynomial surface function is confirmed.

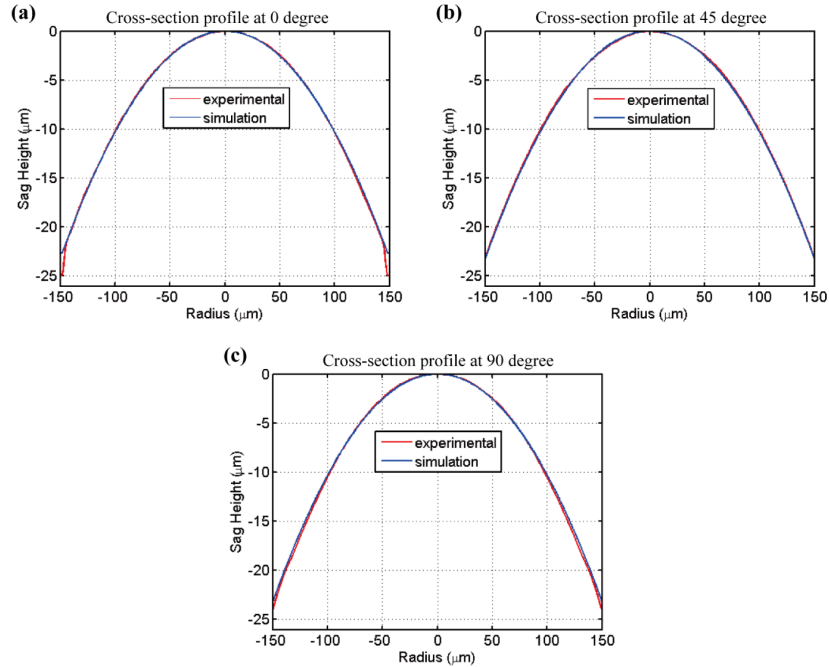


Fig. 6. Comparison of experimental cross-section profiles and simulated profiles at 0°, 45° and 90° relative to x-axis.

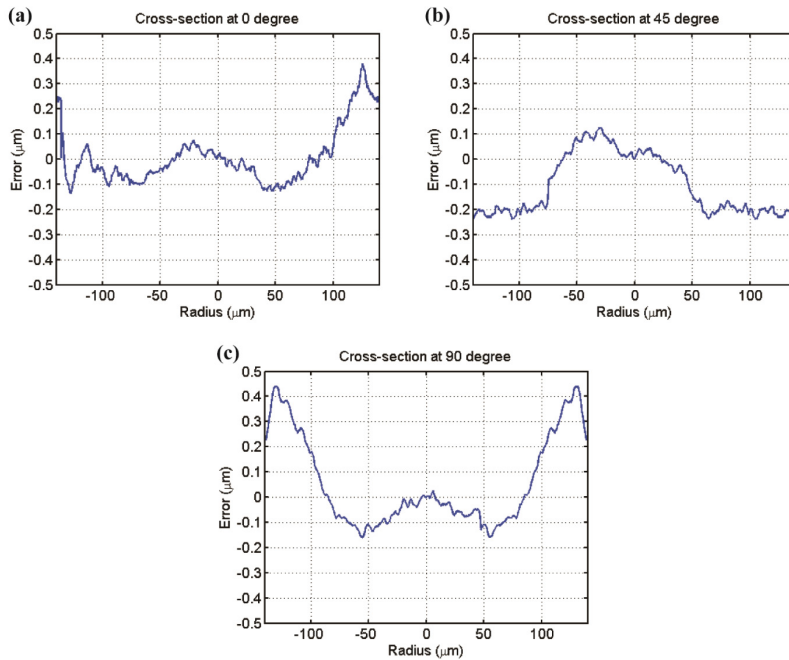


Fig. 7. Difference between experimental cross-section profiles and simulated profiles at 0°, 45° and 90° relative to x-axis.

The surface roughness is critically important for optical components, and must therefore be characterized. The surface roughness of the present fabricated aspherical microlens was measured using an Atomic Force Microscope (SPA-400, Seiko Instruments Inc., Tokyo,

Japan) over an area of size $15 \times 15 \mu\text{m}^2$ located in the central region of the lens. Figure 8 shows that the average surface roughness (R_a) is around 2 nm. In other words, the lens has a mirror-like surface finish.

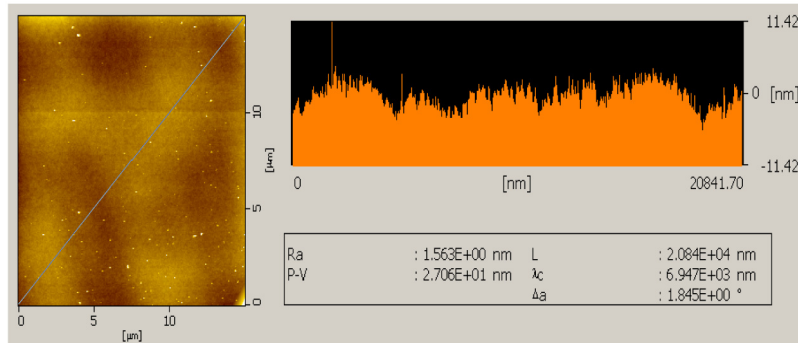


Fig. 8. Surface roughness of fabricated microlens surface profile as measured with Atomic Force Microscope.

C. Laser diode module assembly

Conventional collimated laser beam modules comprise a collimating tube with multiple lenses and a laser diode. As a result, they are physically bulky. Moreover, mounting the lenses in the collimating tube requires the use of expensive apparatus and considerable skill. In aligning the lenses within the tube, it is necessary to carefully control the lens position in four-axial directions (x - y - z - θ) and one tilt-axis (θ_x - θ_y) direction. However, in this study, the aperture and microlens were simply attached to the laser diode window cap using a high bonding strength adhesive (Scotch[®] Super Gluegel, 3M, Minnesota, U.S.). Notably, this approach eliminates the need for z -axis and tilt-axis (θ_x - θ_y) alignment. Thus, in aligning the aperture and microlens with the laser beam center, only three axes (x - y - θ) need to be adjusted. The alignment process was performed using a two-axis (x - y) manual translation stage with an extended holder to hold the aperture or microlens and the θ -axis manual rotary stage of an optical microscope.

4. Results and discussion

A. Spot size measurement

The focused spot size of the machined microlens was measured using an optical microscope (Nikon MM-400/SL, Japan) fitted with a 20X objective lens and a built-in CCD camera. The glued laser diode, aperture and microlens assembly was placed under the microscope such that the laser light was emitted in the vertical direction. Moreover, the objective lens of the microscope was set to the image plane of the focused laser beam by adjusting the z -axis as required. Figure 9 shows the measured light intensity distribution at the focal plane. It is seen that focused spot sizes of 21.6 μm and 18.2 μm are achieved in the x - and y -axis directions, respectively, at the focal distance of 1.98 mm. It is noted that these values are considerably higher than the simulated values (i.e., 5.32 μm and 4.97 μm).

As mentioned above, the fabricated microlens profiles have a maximum fabrication error of $\pm 0.4 \mu\text{m}$ (see Fig. 7) and a surface roughness of $\pm 2 \text{ nm}$ (see Fig. 8). Moreover, some residual machining particles remain on the lens surface. Furthermore, a slight alignment error exists between the laser diode and the circular aperture and microlens. In addition, after passing through the circular aperture, the beam experiences diffraction effect, which causes aberration in the focal plane. Thus, the light cannot be focused to the smallest theoretical spot size predicted in the simulations. To overcome this difficulty, the separation distance between successive laser pulses should be reduced. However, this increases the machining time. Furthermore, the alignment error can be minimized by adopting motorized stage movement

for the two-axis (x-y) alignment process. Nonetheless, in general, the results show that the excimer laser biaxial dragging method with a polynomial surface function provides a feasible approach to fabricate an aspherical microlens to achieve minimum focused spot size.

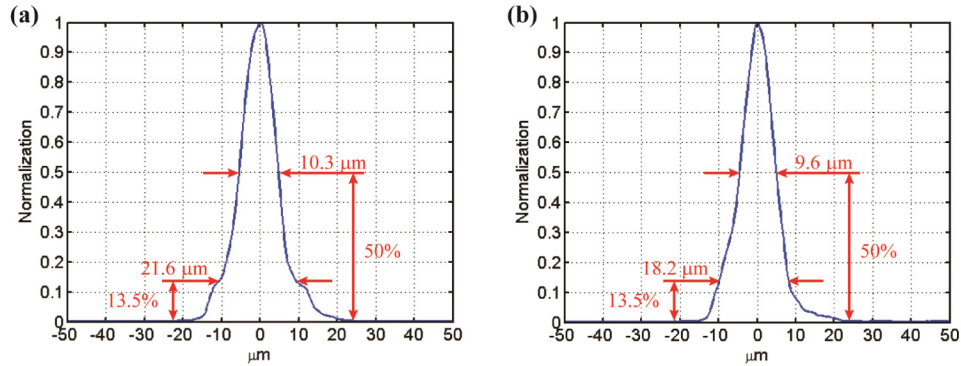


Fig. 9. (a) Experimentally measured light intensity distribution at focal plane and focal spot sizes. (a) Spot size at 13.5% and 50% intensity in x-axis. (b) Spot size at 13.5% and 50% intensity in y-axis.

B. Application of laser diode module in beam pen lithography

To evaluate the real spot size of the focused laser diode beam in practical applications, a B270 glass substrate was uniformly coated with a layer of positive Photo Resist (PR) (S1813, Shipley Company, USA) using a spin coater at a speed of 3000 rpm. The PR-coated substrate was soft-baked at a temperature of 115°C for 60 sec and was then exposed by the laser diode module for 15 ms. Finally, the glass substrate was immersed in a developer solution (MF-319, Shipley Company, USA) for 60 sec. The final PR thickness and spot size were measured using a 3D topography laser scanning system. Figures 10(a) and 10(b) show the 3D topography of the exposed PR layer and the 2D cross-section profile of the developed PR structure, respectively. It is seen in Fig. 10(b) that the average PR layer thickness is 1.89 μm and the spot diameter is 7.8 μm.

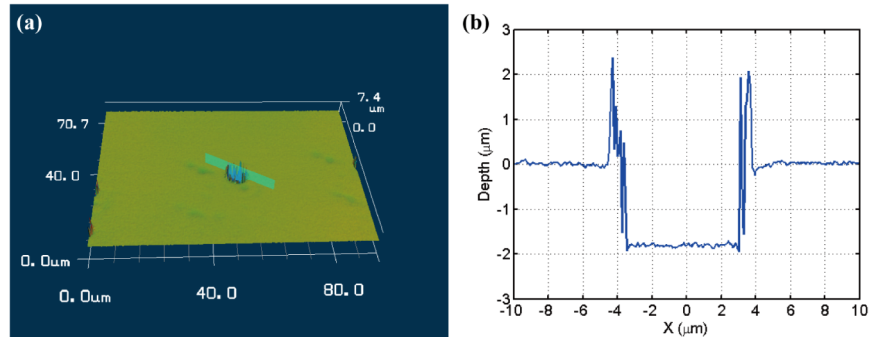


Fig. 10. (a) 3D topography of exposed PR layer. (b) 2D cross-section profile of developed PR structure.

To investigate the smallest attainable PR structure, the laser diode module was used in conjunction with a manual translation stage with three-axis (x-y-z) movement to perform single exposure tests using different focusing distance and exposure times. More specifically, dotted patterns were produced in which the exposure time was progressively increased from 5 to 30 ms along the x-axis direction and focusing distance was increased from 1.90 to 2.2 mm along the y-axis direction. Having patterned the dotted feature, an electron beam thermal evaporation technique (VTI-10CE, ULVAC, Japan) was used to deposit a 50 nm thick gold

metal film on the PR layer. The PR was then removed by a lift-off process. Figure 11(a) shows an SEM image of the metal dots formed with exposure time of 10, 15, 20 and 25 ms along the x-axis direction and focusing distances of 1.96, 1.98 and 2.00 mm along the y-axis direction. Figure 11(b) shows an SEM image of the smallest feature size obtained with an exposure time of 5 ms and a focusing distance of 1.98 mm. The smallest metal-dot dimensions are seen to be $2.57\ \mu\text{m}$ and $2.17\ \mu\text{m}$ in the x- and y-axis directions, respectively.

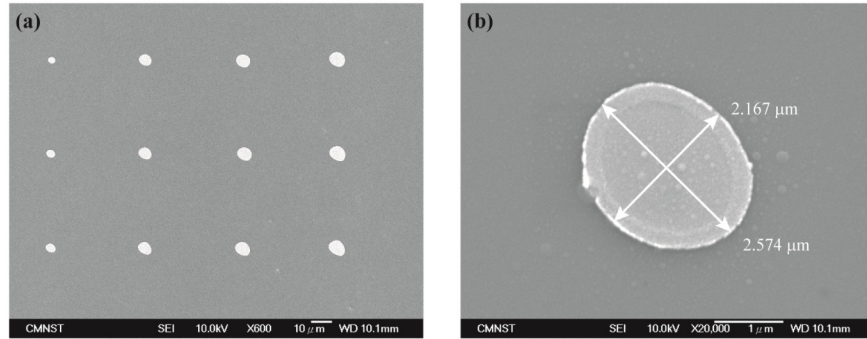


Fig. 11. (a) SEM image of metal-dot patterns. (b) SEM image of smallest metal-dot pattern.

To demonstrate the ability of the laser diode module to realize continuous patterns, two motorized stages (Sigma Koki Co., Tokyo, Japan) were used to translate the substrate in the x- and y-axis directions under the control of a Labview program. Two types of continuous pattern were considered, namely straight-line and spiral. In performing the patterning process, the velocity was varied in the range of 500 to 1000 $\mu\text{m/s}$ along the x-axis direction while the focusing distance was maintained at a constant 1.98 mm. Figure 12(a) shows an SEM image of the straight lines formed given at velocities of 850, 900, 950 and 1000 $\mu\text{m/s}$, respectively. From inspection, the smallest line-width is equal to $3.05\ \mu\text{m}$, and is obtained using a velocity of 1000 $\mu\text{m/s}$. It is noted that this width is slightly larger than the smallest feature size (see Fig. 11(b)). Figure 12(b) shows an SEM image of the spiral pattern obtained using the same velocity of 1000 $\mu\text{m/s}$. The line-width is found to be $4.35\ \mu\text{m}$. In general, the results presented in Figs. 11 and 12 confirm the feasibility of the proposed method for beam pen lithography pattern writing applications.

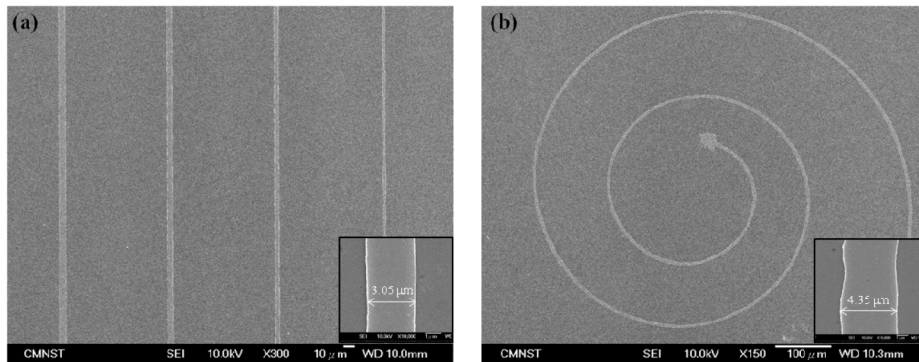


Fig. 12. (a) SEM image of continuous line patterns. (b) SEM image of spiral pattern.

5. Conclusions

This paper has presented an innovative technique for focusing and minimizing the spot size of an elliptically-shaped laser diode beam by means of a circular aperture and an aspherical microlens for use in mask-less beam pen lithography applications. The proposed microlens

has been designed and optimized by means of Zemax simulations, in which a polynomial surface functions is used to prevent axial symmetrical errors and better lens profile. The output surface of the microlens has different profiles in the x- and y-axis directions and is fabricated using an excimer laser dragging method; resulting in a mirror-like surface finish. Importantly, the lens is assembled with the circular aperture and the laser diode using simple adhesive. Consequently, the alignment problem inherent in assembling collimating tubes is avoided. The minimum focused spot size has been evaluated both numerically and experimentally. The feasibility of the proposed microlens for beam pen lithography applications has been demonstrated by patterning dotted, straight-line and spiral features on a glass substrate coated with a thin PR layer followed by electron beam thermal evaporation and a metal lift-off process. The results have shown that dotted features with dimensions of 2.57 μm and 2.17 μm in the x- and y-axis directions, respectively, can be achieved using an exposure time of 5 ms and a focal distance of 1.98 mm. Moreover, continuous patterns like straight-line and spiral patterns with smallest line-widths are 3.05 and 4.35 μm , respectively, have also been presented. Thus, the method proposed in this study has significant potential for writing high-resolution patterns (dotted, line, spiral, alpha-numeric characters and so on) using the beam pen lithography technique.

Acknowledgments

The work is supported by the National Science Council (NSC) and Ministry of Science and Technology (MOST) in Taiwan under grants NSC-103-2120-M-006-005, MOST-103-2622-E-006-030-CC2, and MOST-103-3113-E-006-005.